

Supporting Information Material

Bi₂O₃ nanoparticles encapsulated in surface mounted metal-organic frameworks thin films

Wei Guo¹, Chen Zhi², Chengwu Yang¹, Tobias Neumann², Christian Kübel^{2, 3}, Wolfgang Wenzel²,
Alexander Welle^{1, 3}, Wilhelm Pfleging^{3, 4}, Osama Shekhah⁵, Christof Wöll¹, Engelbert Redel*¹

¹Karlsruhe Institute of Technology, Institute of Functional Interfaces (IFG), Hermann-von-Helmholtz-Platz
1, 76344 Eggenstein-Leopoldshafen, Germany

²Karlsruhe Institute of Technology, Institute of Nanotechnology (INT), Hermann-von-Helmholtz-Platz 1,
76344 Eggenstein-Leopoldshafen, Germany

³Karlsruhe Institute of Technology, Karlsruhe Nano Micro Facility (KNMF), Hermann-von-Helmholtz-Platz
1, 76344 Eggenstein-Leopoldshafen, Germany

⁴Karlsruhe Institute of Technology, Institute of Advanced Materials (IAM), Hermann-von-
Helmholtz-Platz 1, 76344 Eggenstein-Leopoldshafen, Germany

⁵Advanced Membranes and Porous Materials Center, King Abdulah University of Science and
Technology, Kingdom of Saudi-Arabia

Materials and Methods:

X-ray Diffraction (XRD): Each sample was characterized by using a Bruker D8 Advance equipped with a Si-strip detector (PSD Lynxeye©; position sensitive detector) with Cu K_{α1,2} radiation ($\lambda = 0.15418$ nm) in θ - θ geometry, variable slit on primary circle. Scans were run over various ranges with step width of 0.024° 2θ and 84 seconds, for higher order peaks up to 336 seconds per step. The 2θ angle scanning range to observe corresponding peak to deposited film is picked 5° to 60° .

Infrared reflection absorption (IRRA) spectroscopy: IRRA spectra were measured using the infrared spectrometer (Bruker VERTEX 80) purged with dried air. The spectra were recorded in grazing incidence reflection mode at a fixed angle of incidence of 80° relative to the surface normal using mercury cadmium telluride (MCT) detector. Perdeuterated hexadecanethiol SAM on Au/Ti/Silicon substrates were used for reference measurements.

Scanning electron microscopy (SEM): HR-SEM cross-sectional measurements have been performed on a Zeiss HR-SEM (Gemini Class) at 3-5 kV to check the continuity, compactness, and homogeneity of the different prepared (loaded and unloaded) HKUST-1 thin films.

Quartz Crystal Microbalance (QCM): A quartz crystal microbalance (QCM) was employed to growth an HKUST-1 SURMOF thin film on a QCM sensor in a clean and well-controlled manner to further perform the uptake BiPh₃ experiments. The QCM sensor was placed in a flow cell (Q-Sense E4). Infiltration with guest

35 molecules was achieved via a stream of liquid through the cell. The grown SURMOF QCM sensor was grown
36 directly on gold wafer, which was functionalization with a 16-mercaptohexadecanoic acid self-assembled
37 monolayer (MHDA SAM). SURMOF growth was carried out in situ in the QCM flow cell by alternating
38 between the metal source solution (1 mM copper(II) acetate), a solution of 0.2 mM 1,3,5-benzenetricarboxylic
39 acid (BTC) in ethanol and pure ethanol as described previously.

40 The *UV-Vis spectra* were recorded in the range of 200 nm to 800 nm by means of a Cary5000 spectrometer
41 with a UMA unit from Agilent. The UV-Vis spectra of the SURMOFs on the quartz substrate were measured
42 in transmission mode.

43 *Transmission electron microscopy (TEM)*: Plane-view measurements have been performed using an image
44 aberration corrected FEI Titan 80-300 operated at 300 kV and equipped with a Gatan US1000 CCD camera
45 for TEM and SAED analysis and a Fischione HAADF detector for STEM imaging. An EDAX S-UTW
46 detector was used for EDX analysis. The SAED and STEM analysis was performed at LN₂ temperatures to
47 reduce electron beam damage of the HKUST-1. For TEM measurement, samples were prepared by remove
48 the Bi₂O₃@HKUST-1 thin films from quartz-glass sample surface through a laser ablation-process (see Fig.
49 S1) and transfer the thin films onto a holey carbon Au grid (Quantifoil GmbH).

50 *Laser-Ablation Process*: Bi₂O₃@HKUST-1 has been directly grown on HR-TEM grids or was deposited as
51 crystal-pieces through a laser micromachining process. The latter approach was performed by laser lift-off
52 initiated by selective laser ablation using an excimer laser radiation source operating at a wavelength of
53 248 nm with a pulse length of 5 ns.¹

54 *Molecular modeling simulations* were performed using a Monte Carlo algorithm implemented in the
55 simulation package SIMONA with Lennard-Jones and Coulomb interaction. For details on geometry
56 optimization (using DFT) and the force field parameters, see reference. The Lennard-Jones parameters of Bi
57 were set to 1.7295 kcal/mol and 2.8 Å.²

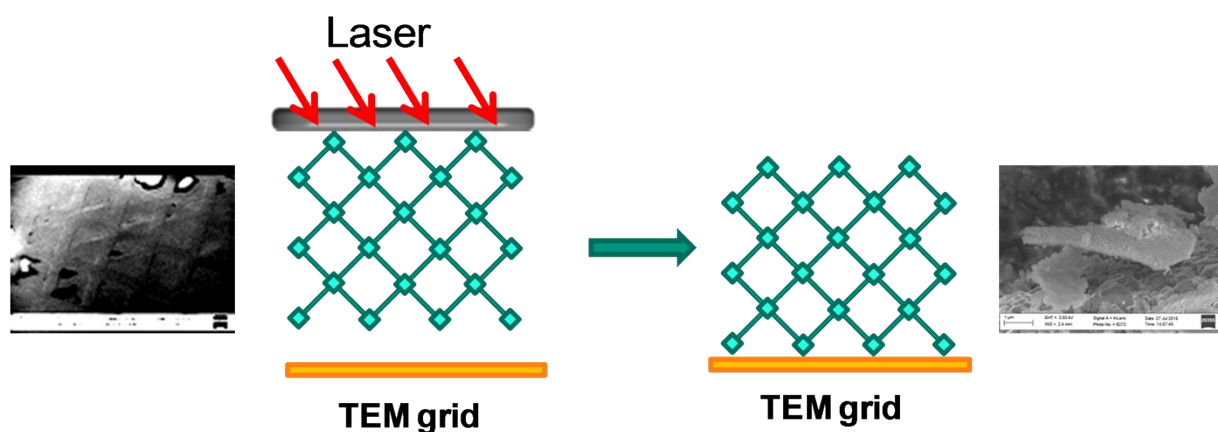
58 *Time-of-flight secondary ion mass spectrometry (ToF-SIMS)* was performed on a TOF.SIMS 5 instrument
59 (ION-TOF GmbH, Münster, Germany). For all experiments a short pulse width (2 ns) 20 keV C₆₀⁺ ion beam
60 was applied as analysis beam. For quasi-static SIMS this beam was rastered over 500×500 μm² and the dose
61 density was limited to below 10¹¹ ions/cm² (static limit). For dynamic SIMS, an additional O₂⁺ beam (500 eV)
62 was applied for erosion of a 450×450 μm² field with a concentric analysis field of 250×250 μm². Spectra
63 calibration was performed on C, Cu, Bi, and Bi₃O₄ peaks, mass deviations were below 20 ppm.

64 *Electrospray ionisation mass spectrometry (ESI-MS)* was

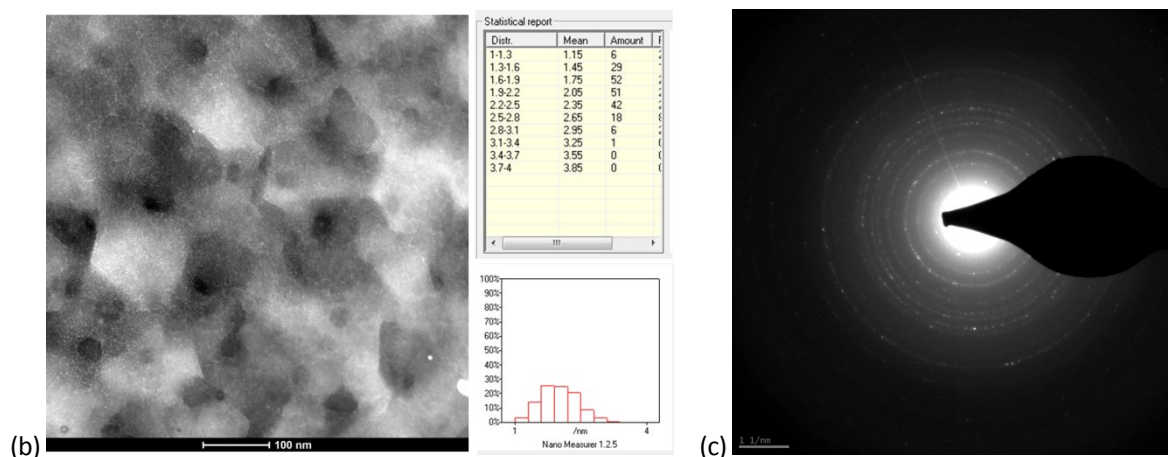
65 The Bi₂O₃ thin film sample for the XPS measurement was grown on the silicon wafer using the liquid
66 deposition method. The deposition solution was using the BiPh₃ solution which after irradiated with 255 nm
67 UV light for 5 h.

68 All HKUST-1 SURMOFs used in the present work were grown on modified Au substrates using the liquid-

69 phase epitaxy (LPE) method,¹ except parts of TEM and UV-vis samples were grown on quartz glass. The
 70 surface modification was carried out by depositing a SAM (self-assembled monolayer) made from 16-
 71 mercaptohexadecanoic acid (MHDA, 99%, Aldrich). The SURMOFs were fabricated using a spray system, as
 72 described in detail in an earlier publication.³ The spray times were 15 s for the copper acetate solution and 25
 73 s for the BTC solution. Each spray step was followed by a rinsing step (3 s) with pure ethanol to remove
 74 residual reactants. A total of 20-35 growth cycles were used for all SURMOFs investigated in this work.
 75 Before further processing, all SURMOFs samples were activated by ultrasound in dichloromethane solution
 76 for 5 min to remove residual solvent from the SURMOFs pores and characterized by X-ray diffraction (XRD)
 77 (see Fig. 2b). Cross-sectional images recorded by scanning electron microscopy (SEM) demonstrate that the
 78 thickness of SURMOFs amounts to about 100 nm (see also Fig. S2). For BiPh₃ loading, a HKUST-1
 79 SURMOF was placed into a 250 ml flask, which was then evacuated to 200 Pa at room temperature (RT) for
 80 30 min. Subsequently, a freshly prepared solution of BiPh₃ (triphenylbismuth) in ethanol (1 mM, Aldrich)
 81 was injected quickly into the reaction flask and heated to 65°C for 36 h. BiPh₃ is a simple organo-bismuth
 82 compound which is quite stable under normal conditions.⁴ The loading of BiPh₃ into the HKUST-1
 83 SURMOFs was analyzed in a quantitative fashion using a quartz crystal microbalance (QCM) (see Fig. S3).
 84 The mass density of the activated framework amounts to 0.98 g•cm⁻³, which is increased by the ethanol
 85 contained in the pores, yielding a total mass-density of the ethanol-soaked HKUST-1 of 1.53 g•cm⁻³.⁵ A
 86 quantitative analysis of the QCM-data yields a BiPh₃ loading of ~ 0.17 g BiPh₃ per 1 g ethanol-soaked
 87 HKUST-1. This corresponds to a loading of 2-3 BiPh₃ molecules per HKUST-1 unit cell. After loading BiPh₃,
 88 the reaction flask with BiPh₃@HKUST-1 sample was taken out from the oven and irradiated with 255 nm UV
 89 light for 5 h. Upon irradiation, the solution turns from clear to opaque (Fig. S4). Subsequently, the sample was
 90 removed from the reaction solution, rinsed with pure ethanol and dried in dry N₂ gas. Then, the sample was
 91 irradiated with 255 nm UV light for 1 h.

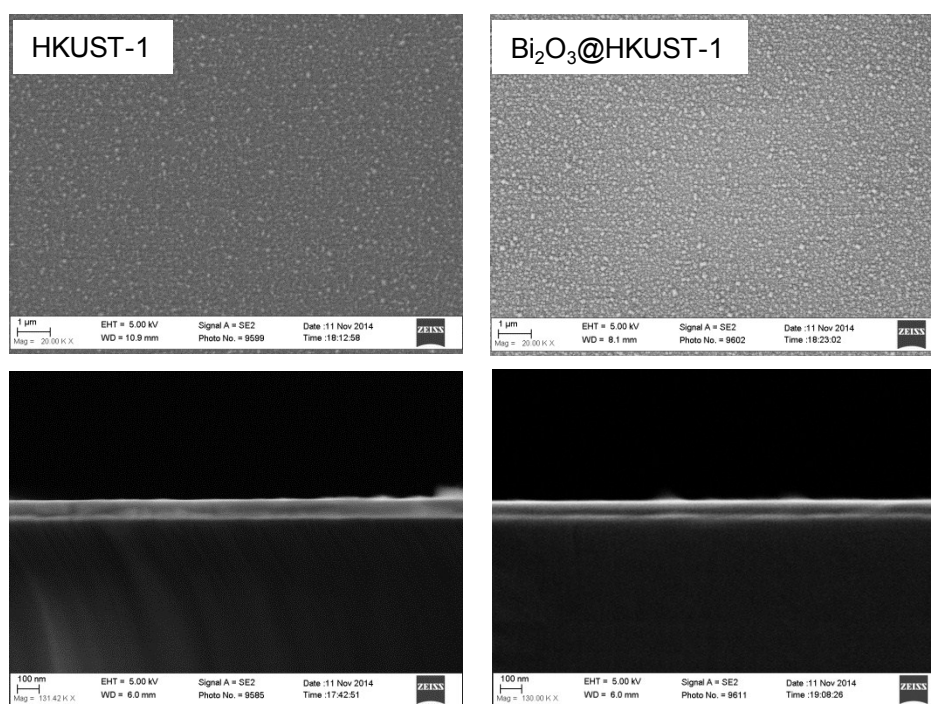


(a)



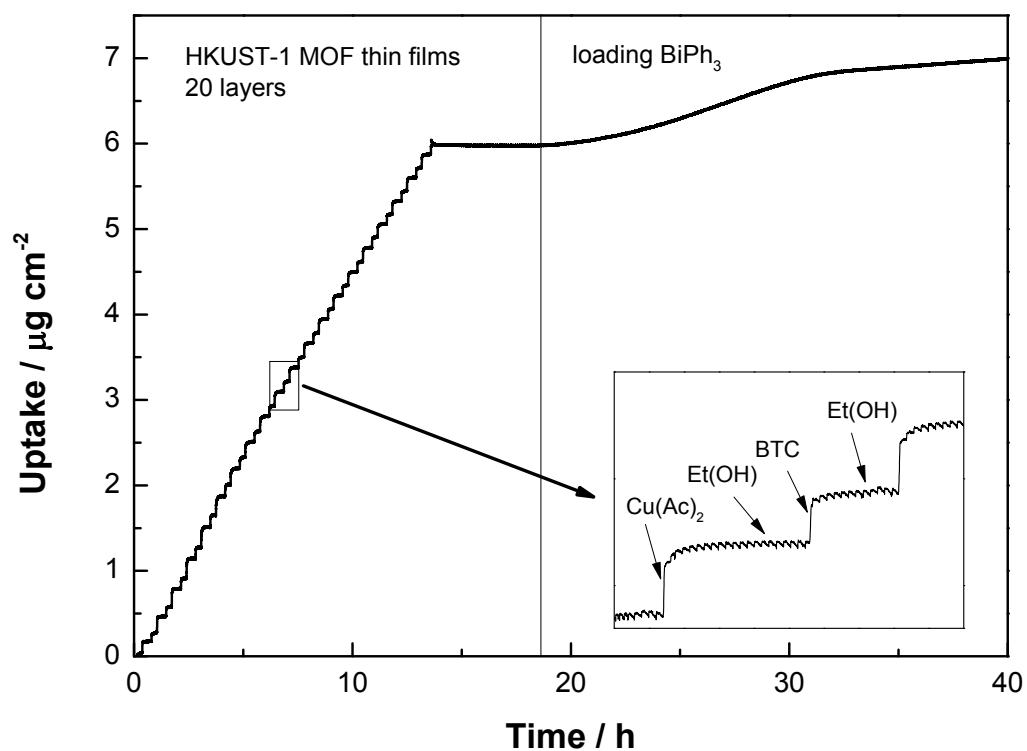
95
96

97 Figure S1. Synthesis scheme of the Bi_2O_3 @HKUST-1 SURMOFs TEM sample preparation by a laser ablation process.
98 b) HR-TEM of embedded Bi_2O_3 NPs in the surface of oriented HKUST-1 SURMOF. (c) cryo-SAED diffraction pattern
99 of deposited HKUST-1 thin films, see also TableS1.



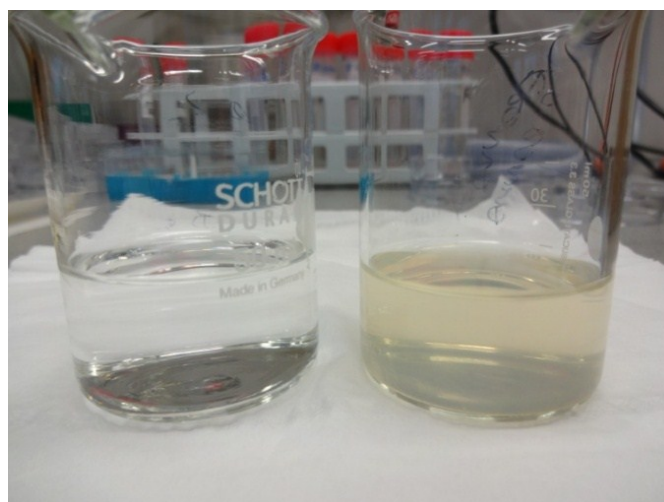
100

101 Figure S2. Scanning electron micrograph (SEM) of 20 cycles of $\text{Cu}_3(\text{BTC})_2$ MOF thin films (left) and after loading Bi_2O_3
102 (right).



103

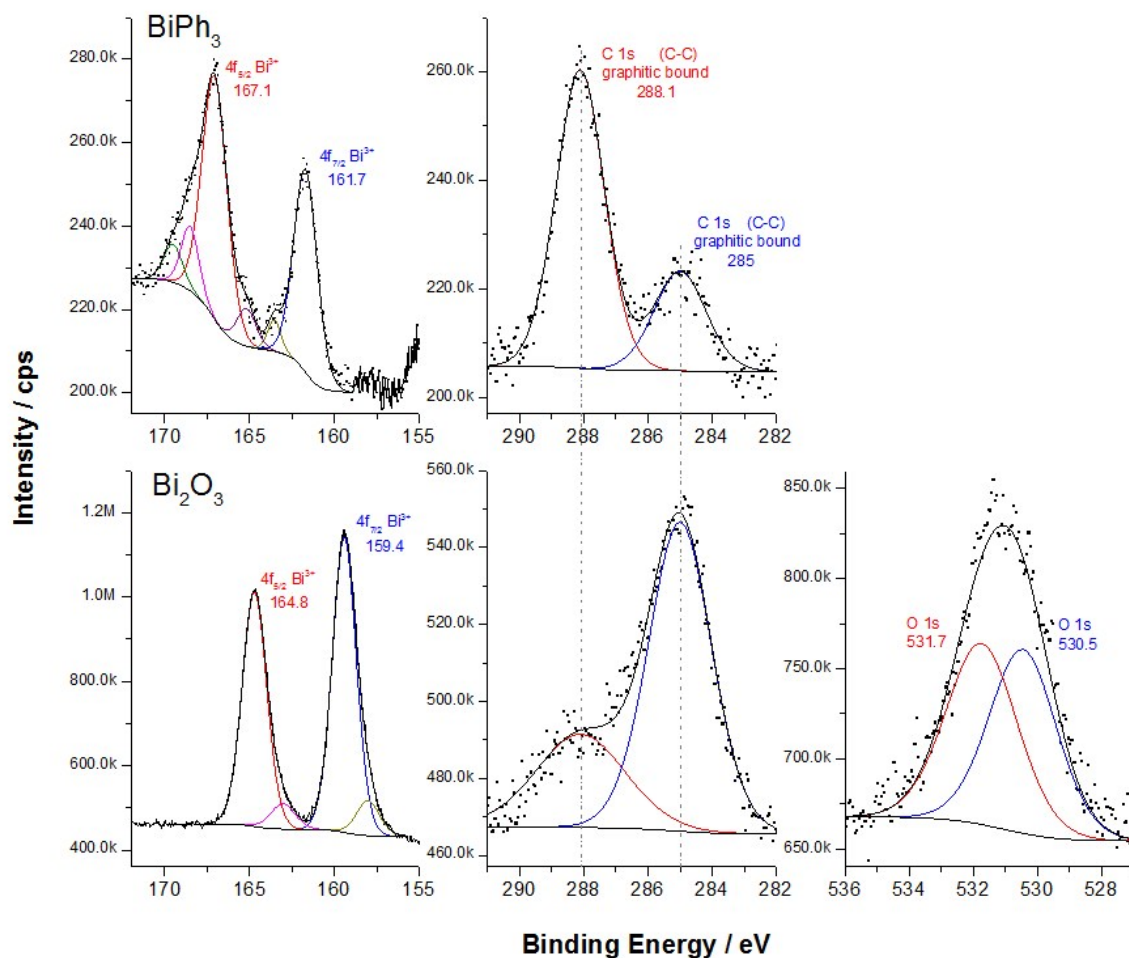
104 Figure S3. Layer-by-layer growth of the HKUST-1 SURMOF on the QCM sensor with 20 cycles and performed
 105 uptake experiment with BiPh₃. The inset is a magnification of the layer-by-layer growth of the SURMOF. (The
 106 small oscillations in the curve is from the pump)



107

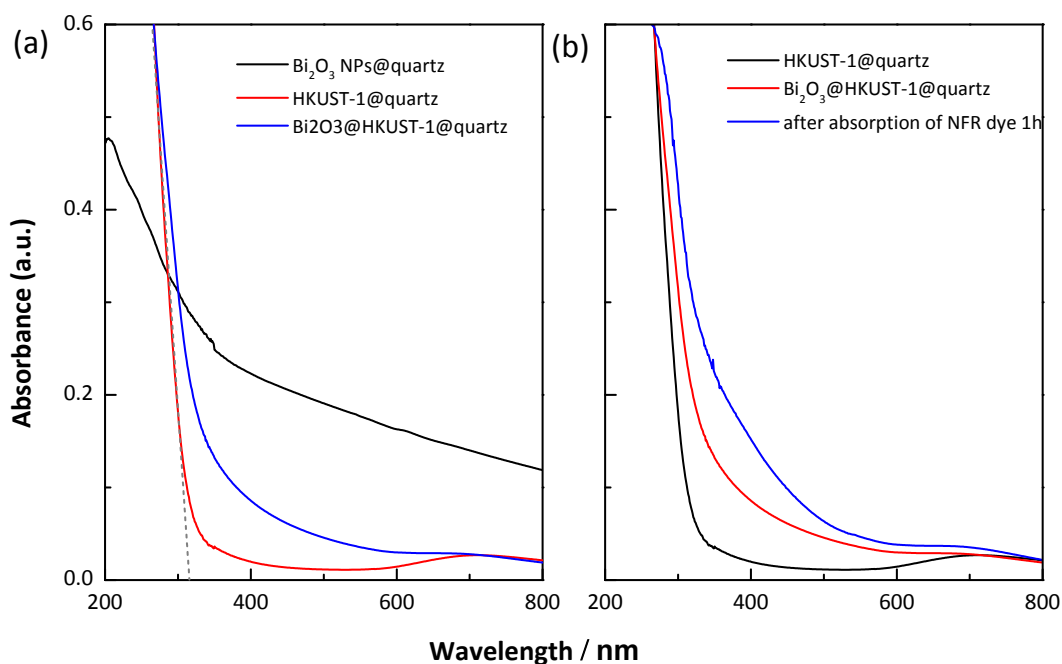
108 Figure S4. BiPh₃ ethanolic solution before irradiation (left) and after irradiation (right).

109



110

111 Figure S5. X-ray photoelectron spectrum (XPS) analysis for BiPh₃ (up) and Bi₂O₃ (down).



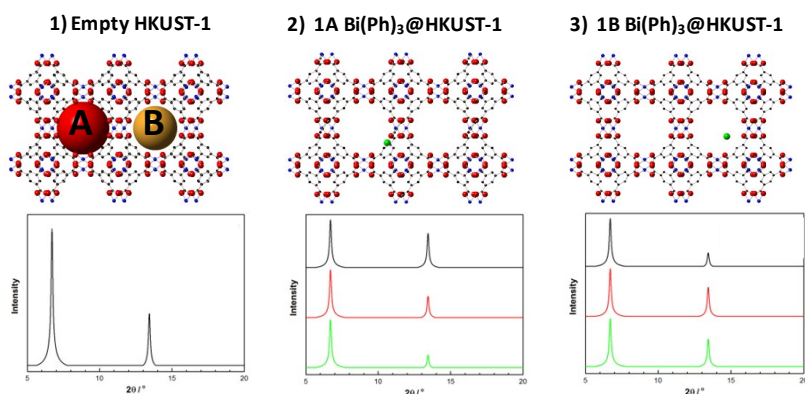
112

113 Figure S6. (a) UV-Vis absorption spectra of the Bi₂O₃ thin films on quartz glass (black), HKUST-1 SURMOFs (red) and

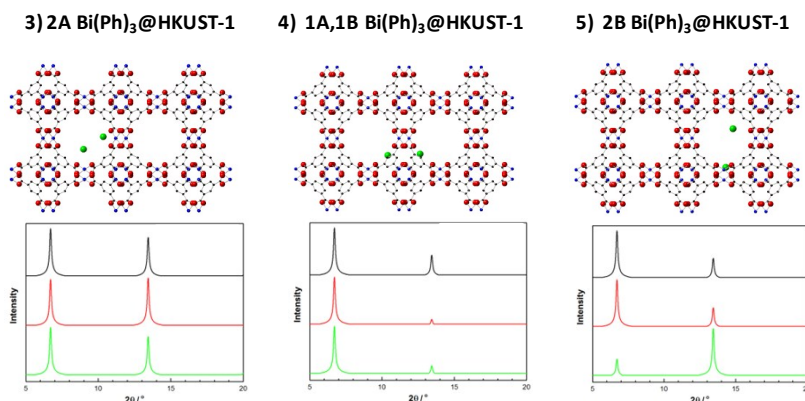
114 Bi₂O₃@HKUST-1 SURMOFs (blue). (b) UV-Vis absorption spectra of HKUST-1 SURMOFs (black), Bi₂O₃@HKUST-1

115 SURMOFs (red) and Bi_2O_3 @HKUST-1 SURMOFs after absorption of NFR dye 1 h (blue).

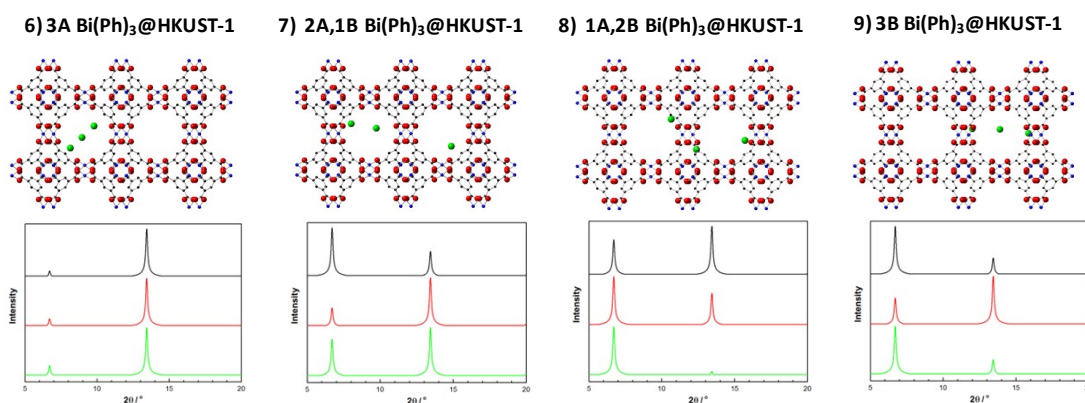
1 BiPh_3 @HKUST-1



2 BiPh_3 @HKUST-1

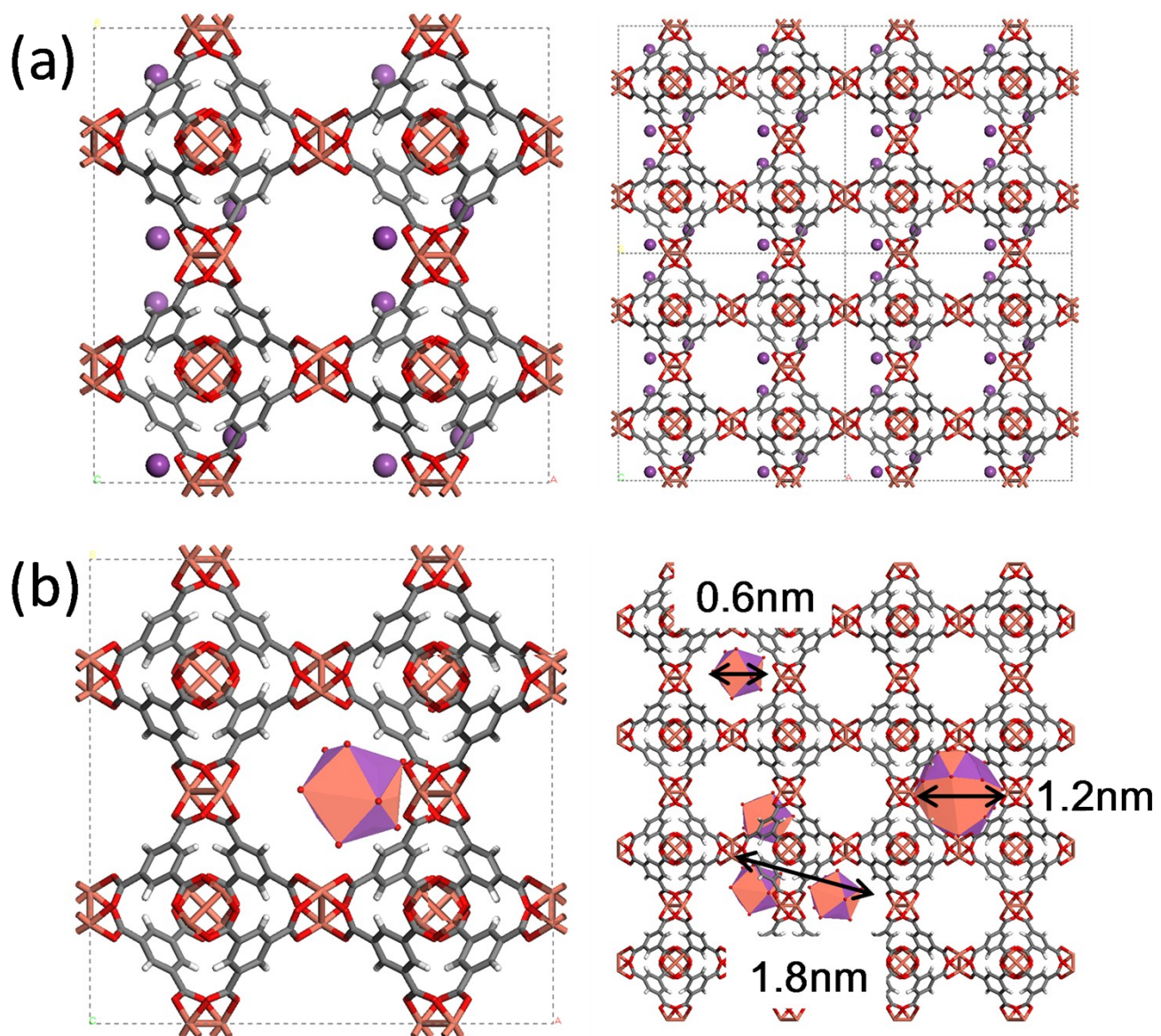


3 BiPh_3 @HKUST-1



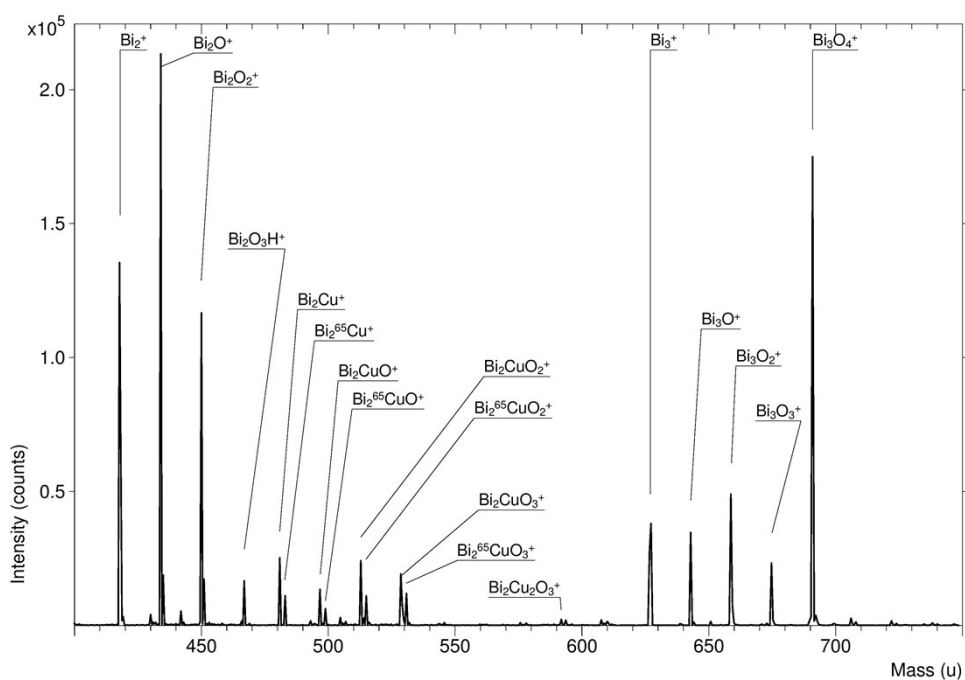
116

117 Figure S7. Schematic structure of HKUST-1 (1) (large pore: A, middle pore: B) and after loading different number
 118 [single Bi^{3+} in A (1), single Bi^{3+} in B (2), 2 Bi^{3+} in A (3), 1 $\text{Bi}(\text{Ph})_3$ in A and 1 Bi^{3+} in B (4), 2 Bi^{3+} in B (5), 3 Bi^{3+} in A (6),
 119 2 Bi^{3+} in A and 1 Bi^{3+} in B (7), 1 Bi^{3+} in A and 2 Bi^{3+} in B (8), 3 Bi^{3+} in B (9)]. Calculated X-ray diffraction patterns for
 120 HKUST-1 before and after loading Bi^{3+} in different plane [(001) plane (up, black line), (010) plane (middle, red line)
 121 and (100) plane (down, green line)]. The anion was hidden.



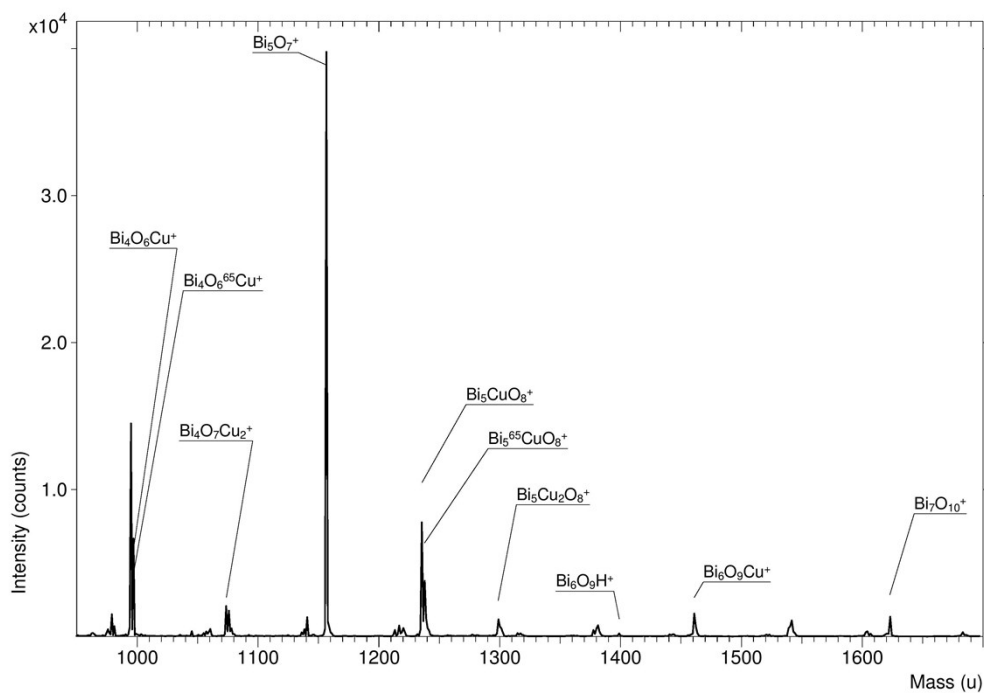
122

123 Figure S8. a) Infiltration of three BiPh₃ molecules inside an HKUST-1 pore. b) Model of photosynthesized (Bi₂O₃)_n
 124 Clusters/NPs with $n = 1-5$ in the defined pore-space of HKUST-1, avoiding sintering with particles from adjacent
 125 pores.



126

127 Figure S9. Quasi-static SIMS of a Bi_2O_3 @HKUST-1 SURMOF stack performed with C_{60} (20 keV) bunched. $400 < m/z$
 128 < 750 .

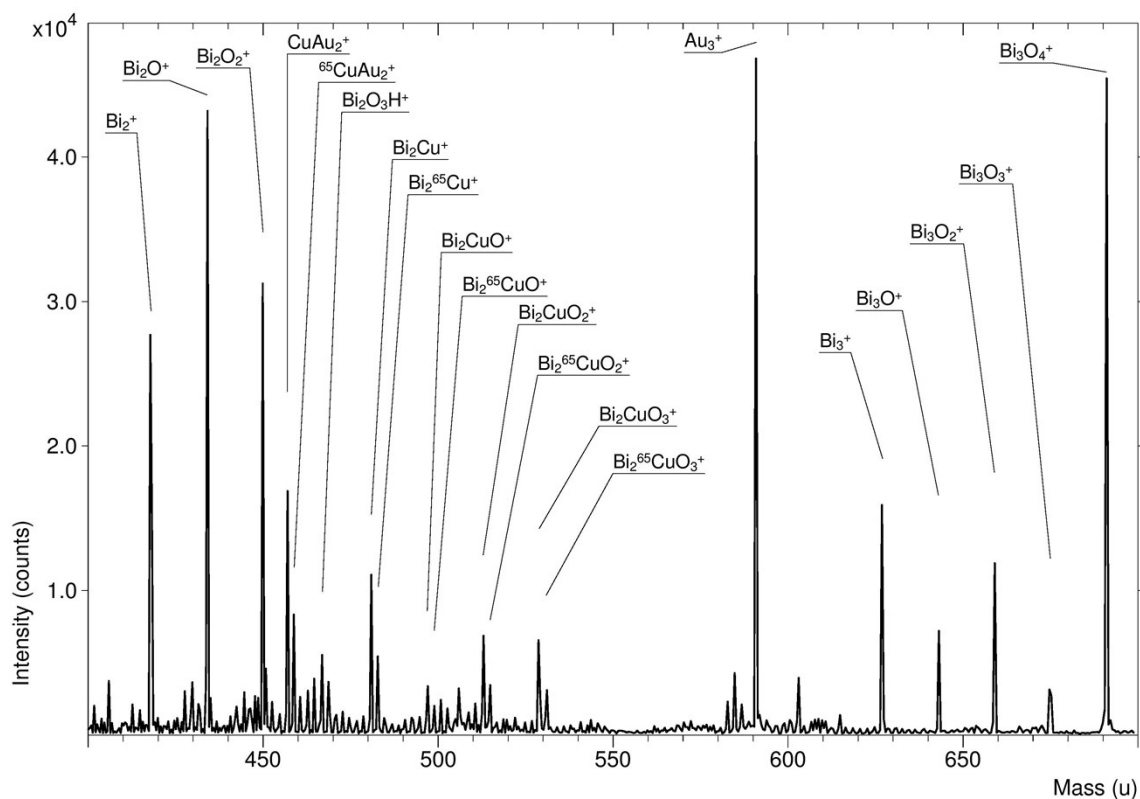


129

130 Figure S10. Quasi-static SIMS of a Bi_2O_3 @HKUST-1 SURMOF stack performed with C_{60} (20 keV) bunched. $950 <$

131 $m/z < 1700$

132 As shown in Figs. S9 and S10, the positive polarity secondary ion mass spectrum obtained under quasi-static
133 conditions from a Bi_2O_3 @HKUST-1 SURMOF stack is dominated by several bismuth oxides and $\text{Bi}_x\text{O}_y\text{Cu}_z$ cluster
134 ions. The bismuth oxide fragment Bi_2O shows highest intensity (212 kcts) followed by Bi_3O_4 (170 kcts), Bi_4O_5 17
135 (kcts), and Bi_5O_7 (39 kcts). A marked drop in intensity is observed for bismuth oxide clusters bigger than Bi_5O_7 .
136 Bi_6O_9 is not detectable, Bi_7O_{10} has an intensity of only 1 kcts.



137

138 Figure S11. Dynamic SIMS of a Bi_2O_3 @HKUST-1 SURMOF stack performed with C_{60} (20 keV, 0.1 pA) bunched
139 analysis beam and O_2 (500 eV, 110 nA) sputter beam. $400 < m/z < 700$.

140 Under dynamic SIMS conditions, using a high current oxygen sputter beam to erode the surface of a
141 Bi_2O_3 @HKUST-1 SURMOF stack gold peaks from the substrate appear and new cluster ions like CuAu_2 are formed
142 due to the mixing process during ion bombardment.

143

144

145

146

147

148 Table S1: SAED (Selected Area Electron Diffraction) data and lattice spacing (d) for comparison between electron
149 diffraction and XRD data of [111] oriented HKUST-1.

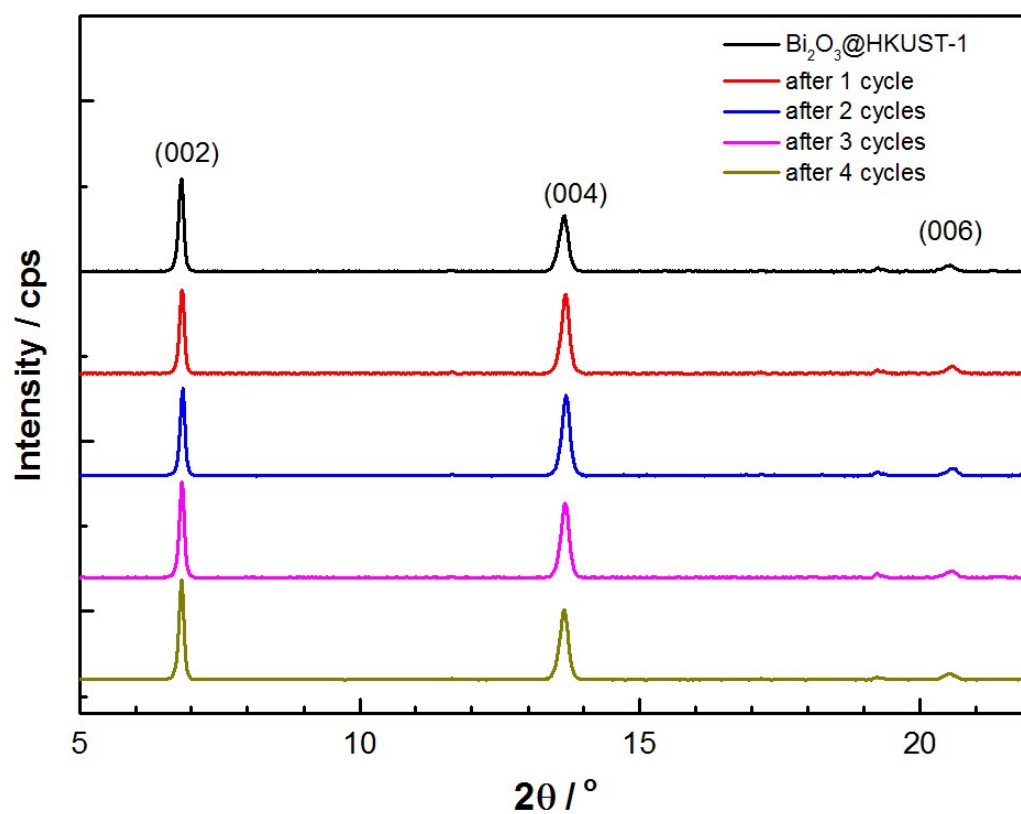
	SAED d [nm]	HKUST [111] d [nm]			
		H	K	L	
	0.915	0.93	2	2	0
		0			
	0.547	0.53	2	2	4
		7			
	0.470	0.46	4	4	0
		5			
	0.359	0.35	2	4	6
		1			
	0.310	0.31	6	6	0
		0			
	0.265	0.26	4	4	8
		8			
	0.222	0.21	6	4	1
		3			0

150

151

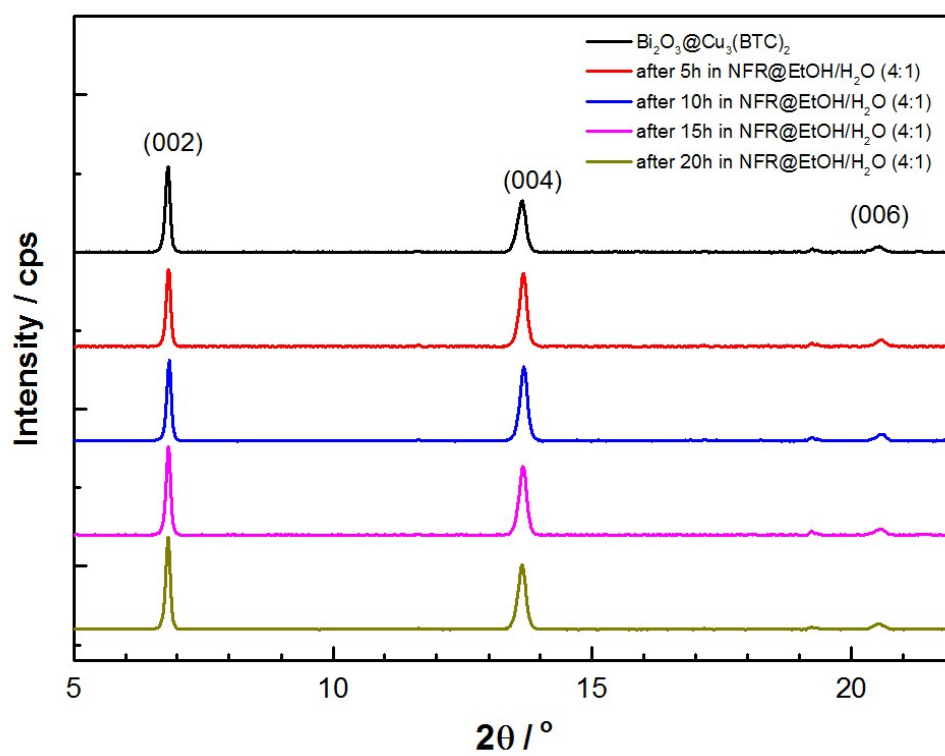
152

153



154

155 Figure S12. XRD patterns for $\text{Bi}_2\text{O}_3@HKUST-1$ SURMOF before and after reaction.



156

Figure S13. XRD patterns for Bi₂O₃@HKUST-1 SURMOF in NFR@EtOH/H₂O solution for different times.

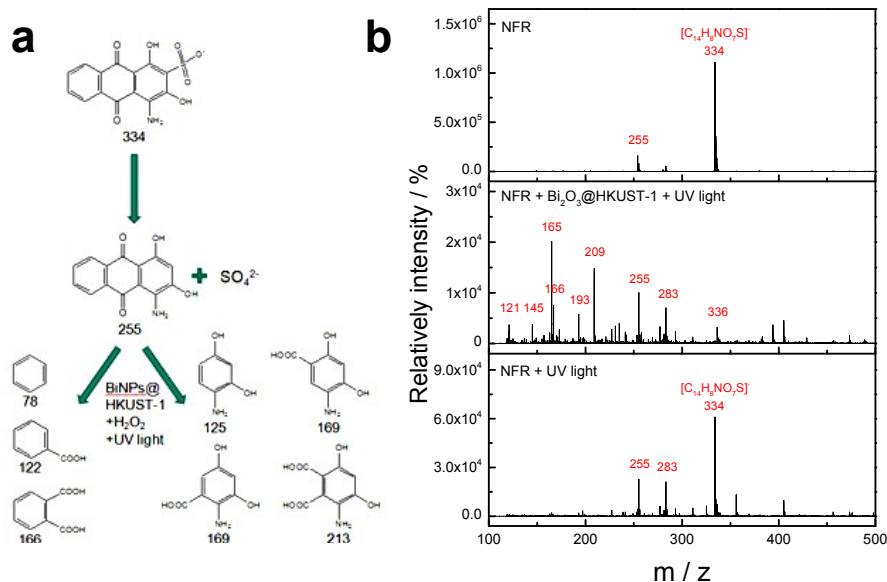


Figure S14. (a) Proposed degradation pathway of NFR using the Bi₂O₃@ HKUST-1 SURMOF for the photodegradation of NFR under UV light irradiation. (b) ESI-MS of the NFR solution (top), NFR solution after UV light exposure with Bi₂O₃@HKUST-1 SURMOF (middle), and NFR solution after UV light exposure without any catalyst (bottom). As shown in Figure S14, the application of the Bi₂O₃@HKUST-1 SURMOF catalysis system leads to an efficient photodegradation of the parent compound, NFR, and to an enhanced formation of smaller photodegradation products.

References

- 1 W. Pfleging, R. Kohler, I. Südmeyer and M. Rohde, *Springer Series in Materials Science*, 2013, 161, 319.
- 2 A. Maulana, Z. Suud, K.D. Hermawan, etc, *Prog. Nucl. Energ.*, 2008, 50, 616-620.
- 3 H. K. Arslan, O. Shekhah, D. C. F. Wieland, M. Paulus, C. Sternemann, M. A. Schroer, S. Tiemeyer, M. Tolan, R. A. Fischer and C. Wöll, *J. Am. Chem. Soc.*, 2011, 133, 8158.
- 4 H. K. Arslan, O. Shekhah, J. Wohlgemuth, M. Franzreb, R. A. Fischer and C. Wöll, *Advanced functional materials*, 2011, 21, 4228.
- 5 L. Heinke, Z. G. Gu and C. Wöll, *Nat Commun*, 2014, 5.